

Alma Mater Studiorum Università di Bologna
Archivio istituzionale della ricerca

Effects of anisotropy on the transition to absolute instability in a porous medium heated from below

This is the final peer-reviewed author's accepted manuscript (postprint) of the following publication:

Published Version:

Celli M., Barletta A. (2022). Effects of anisotropy on the transition to absolute instability in a porous medium heated from below. PHYSICS OF FLUIDS, 34(2), 1-8 [10.1063/5.0085077].

Availability:

This version is available at: <https://hdl.handle.net/11585/872655> since: 2022-02-28

Published:

DOI: <http://doi.org/10.1063/5.0085077>

Terms of use:

Some rights reserved. The terms and conditions for the reuse of this version of the manuscript are specified in the publishing policy. For all terms of use and more information see the publisher's website.

This item was downloaded from IRIS Università di Bologna (<https://cris.unibo.it/>).
When citing, please refer to the published version.

(Article begins on next page)

This is the final peer-reviewed accepted manuscript of:

M. Celli, A. Barletta; Effects of anisotropy on the transition to absolute instability in a porous medium heated from below. *Physics of Fluids* 1 February 2022; 34 (2): 024105.

The final published version is available online at:

<https://doi.org/10.1063/5.0085077>

Terms of use:

Some rights reserved. The terms and conditions for the reuse of this version of the manuscript are specified in the publishing policy. For all terms of use and more information see the publisher's website.

This item was downloaded from IRIS Università di Bologna (<https://cris.unibo.it/>)

When citing, please refer to the published version.

Effects of anisotropy on the transition to absolute instability in a porous medium heated from below

M. Celli^{1, a)} and A. Barletta¹

¹*Alma Mater Studiorum Università di Bologna, Department of Industrial Engineering, Viale Risorgimento 2, 40136 Bologna, Italy*

(Dated: 28 January 2022)

The emerging instability of a forced throughflow in a fluid saturated horizontal porous duct of rectangular cross section is investigated. The duct is heated from below by assuming the horizontal boundaries to be at different temperatures. Both the horizontal and the vertical boundaries are impermeable and the basic flow is parallel to such boundaries. The porous medium is anisotropic with different permeabilities in the vertical and horizontal directions. The effect of the anisotropy on the onset of the buoyancy driven modal instability and absolute instability is analysed. The parametric conditions leading to the instability of the basic flow are determined by employing an analytical dispersion relation. The different permeabilities in the vertical and horizontal directions come out to play opposite roles in the onset of modal instability and in the transition to absolute instability. It is shown that an increasing vertical permeability has a destabilising effect, while an increasing horizontal permeability has a stabilising effect.

I. INTRODUCTION

The onset of convection in a horizontal porous layer heated from below has widespread applications either in engineering and geophysics. Such applications regard, for instance, the dynamics of groundwater reservoirs, the diffusion of pollutants in the soil, the CO₂ sequestration and the thermal insulation of buildings. In several cases, the porous media involved in these applications are anisotropic.

The study reported in this paper contributes further novel findings to the present knowledge on the buoyancy driven instability in fluid saturated horizontal porous layers heated from below¹. This is also well-known as the Darcy–Bénard problem, or as the Horton–Rogers–Lapwood (HRL) problem. In fact, the first investigations on this topic were carried out by Horton and Rogers², and by Lapwood³. These authors considered a porous layer infinitely wide in the horizontal directions and bounded in the vertical direction by two impermeable boundaries held at different temperatures, such that an upward vertical temperature gradient is imposed. By assuming a layer saturated with a motionless fluid, the threshold conditions for the onset of modal instability were evaluated finding that convective cells may arise when the Darcy–Rayleigh number becomes greater than $4\pi^2$. When Prats⁴ further developed the HRL problem by including a basic horizontal throughflow, he found out that the threshold for the onset of modal instability was not affected by the mass flow rate.

Barletta⁵ presents a survey of the recent research studies regarding both the modal instability and the transition to the absolute instability for the Prats problem. While the modal instability analysis is focussed on investigating the evolution in time of single Fourier modes perturbing the whole basic state, the absolute instability analysis deals with the evolution of perturbation wavepackets expressed by a Fourier integral over all possible wavenumbers. The latter type of instability is the one that is typically observed in the laboratory reference frame when a localised disturbance spreads in space and travels in the direction of the basic flow. For this reference frame, amplified perturbations can be detected only when they are not convected downstream by the basic throughflow. By illustrating the transition to absolute instability for the Prats problem, Barletta⁵ points out that the threshold value of the governing parameter, *i.e.* the Rayleigh number, is a monotonically increasing function of the basic flow rate, parametrised through the Péclet number. By increasing the flow rate, or the Péclet number, the unstably growing perturbation is more likely to be convected downstream, so that the basic flow becomes more stable.

An interesting reformulation of the HRL problem accounting for the anisotropy of the porous medium has been performed in several papers^{6–13}. These authors carried out the modal stability analysis assuming the thermophysical properties of the porous media to have constant although different values along the three Cartesian directions. The anisotropy effect on the convection in porous media has been investigated also by Rees, Storesletten, and Bassom¹⁴, Ennis-King, Preston, and Paterson¹⁵, Nield and Kuznetsov¹⁶, De Paoli, Zonta, and Soldati¹⁷.

The analysis presented in this paper is focussed on the

^{a)}corresponding author: michele.celli3@unibo.it

investigation of both modal and absolute instabilities for the Prats problem where an anisotropic porous duct, with a rectangular cross section, is considered. In particular, the porous medium is characterised by two different uniform values of permeability: a value for the permeability in the horizontal directions and a value for the permeability in the vertical direction. This work fills a gap in the literature since, to the best of authors' knowledge, the absolute instability analysis for the anisotropic Prats' problem in a rectangular duct has not been investigated to date.

II. MATHEMATICAL MODEL

A fluid saturated horizontal porous duct of rectangular cross section with height H and width W is considered. This duct is assumed to be unbounded in the x direction, while it is bounded by impermeable walls in the y and z directions. The duct is heated from below with the horizontal boundaries having different temperatures: the boundary at $z = 0$ is held at temperature $T_0 + \Delta T$, with $\Delta T > 0$, while the boundary at $z = H$ is held at temperature T_0 , see Fig. 1.

The momentum transport is formulated by employing Darcy's law together with the Oberbeck-Boussinesq approximation. The energy transport is modelled by assuming a negligible viscous dissipation and local thermal equilibrium between the fluid and solid phases. A scaling is used for the non-dimensional formulation,

$$\begin{aligned} \frac{\mathbf{x}}{H} &\rightarrow \mathbf{x}, & \frac{\chi}{H^2} t &\rightarrow t, & \frac{H}{\chi} \mathbf{u} &\rightarrow \mathbf{u}, \\ \frac{K_z}{\chi \mu} p &\rightarrow p, & \frac{T - T_0}{\Delta T} &\rightarrow T. \end{aligned} \quad (1)$$

Thus, the governing balance equations, in dimensionless form, are given by

$$\begin{aligned} \nabla \cdot \mathbf{u} &= 0, \\ u &= -a \frac{\partial p}{\partial x}, \\ v &= -a \frac{\partial p}{\partial y}, \\ aw &= -a \frac{\partial p}{\partial z} + RT, \\ \sigma \frac{\partial T}{\partial t} + \mathbf{u} \cdot \nabla T &= \nabla^2 T, \end{aligned} \quad (2)$$

with the boundary conditions

$$\begin{aligned} y = 0, s : & \quad v = 0, \quad \frac{\partial T}{\partial y} = 0, \\ z = 0 : & \quad w = 0, \quad T = 1, \\ z = 1 : & \quad w = 0, \quad T = 0. \end{aligned} \quad (3)$$

In Eqs. (1)–(3), p denotes the local difference between the pressure and the hydrostatic pressure (hereafter, p is just called pressure for the sake of brevity), (x, y, z) are the Cartesian components of the position vector \mathbf{x} , (u, v, w) are the Cartesian components of the seepage velocity vector \mathbf{u} , t is the time, T is the temperature, $s = W/H$ is the aspect ratio of the duct and σ is the heat capacity ratio, namely the ratio between the heat capacity per unit volume of the saturated porous medium and the heat capacity per unit volume of the fluid¹. Furthermore, the Darcy–Rayleigh number R is defined as

$$R = \frac{\rho g \beta K_h H \Delta T}{\mu \chi}, \quad (4)$$

where ρ is the fluid density at the reference temperature T_0 , g is the modulus of the gravitational acceleration \mathbf{g} , β is the thermal expansion coefficient of the fluid, μ is the dynamic viscosity of the fluid and χ is the average thermal diffusivity of the fluid saturated porous medium.

We defined R using the horizontal permeability K_h instead of the vertical, K_z , because the definition (4) simplifies the interpretation of the results obtained by the forthcoming absolute instability analysis. We mention that Storesletten⁹ defines the Darcy–Rayleigh number differently by employing K_z instead of K_h .

The quantity χ is defined as the ratio between the average thermal conductivity of the fluid saturated porous medium and the volumetric heat capacity of the fluid, i.e., the product ρc , where c is the specific heat of the fluid. Following the reasoning presented by Beckermann and Viskanta¹⁸ and by Vafai and Kim¹⁹, the thermal dispersion effects have been implicitly taken into account in the average thermal diffusivity χ .

The parameter a is the ratio between the permeability of the porous medium in the horizontal directions, K_h , and the permeability in the vertical direction, K_z , namely

$$a = \frac{K_h}{K_z}. \quad (5)$$

Since Darcy's law is employed to model the momentum transport, the values of K_h and K_z have to be small enough. This constraint implies that the limiting case $a \rightarrow 0$ has to be obtained by assuming $K_h \ll K_z$ with K_z yet sufficiently small in compliance with Darcy's law.

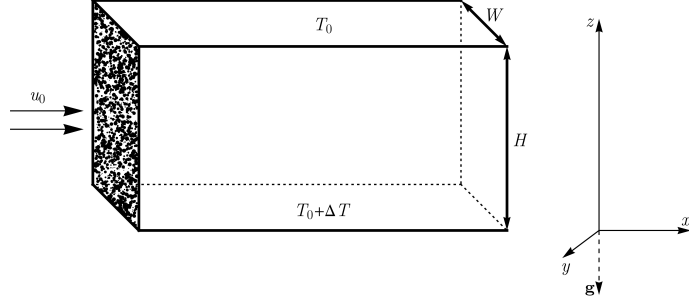


FIG. 1. Sketch of the porous duct geometry and boundary conditions.

III. BASIC STATE

A steady state solution of Eqs. (2) and (3) is given by a uniform velocity profile, with value Pe , in the x direction and a uniform negative temperature gradient in the z direction, namely

$$u_b = Pe, \quad v_b = w_b = 0, \quad T_b = 1 - z, \quad \frac{\partial p_b}{\partial x} = -\frac{Pe}{a}, \quad \frac{\partial p_b}{\partial y} = 0, \quad \frac{\partial p_b}{\partial z} = \frac{R}{a}(1 - z), \quad (6)$$

where the subscript “ b ” indicates that Eq. (6) defines the basic state. The basic state (6) yields a pure conduction regime with the heat flux parallel to the z direction. In Eq. (6), Pe is the Péclet number defined as

$$Pe = \frac{u_0 H}{\chi}, \quad (7)$$

and u_0 is the dimensional basic velocity (see Fig. 1).

namely

$$\begin{aligned} a \frac{\partial^2 p}{\partial x^2} + a \frac{\partial^2 p}{\partial y^2} + \frac{\partial^2 p}{\partial z^2} - \frac{R}{a} \frac{\partial T}{\partial z} &= 0, \\ \sigma \frac{\partial T}{\partial t} - a \frac{\partial p}{\partial x} \frac{\partial T}{\partial x} - a \frac{\partial p}{\partial y} \frac{\partial T}{\partial y} &+ \left(\frac{R}{a} T - \frac{\partial p}{\partial z} \right) \frac{\partial T}{\partial z} = \nabla^2 T, \\ y=0, s: \quad \frac{\partial p}{\partial y} &= 0, \quad \frac{\partial T}{\partial y} = 0, \\ z=0: \quad \frac{\partial p}{\partial z} &= \frac{R}{a}, \quad T = 1, \\ z=1: \quad \frac{\partial p}{\partial z} &= 0, \quad T = 0, \end{aligned} \quad (8)$$

where the impermeability condition in Eq. (3) have been reformulated in terms of the pressure by employing the modified Darcy’s law, Eq. (2). The stability of the basic state (6) is analysed by employing small-amplitude perturbations, *i.e.*,

$$\begin{aligned} p(x, y, z, t) &= p_b(x, z) + \varepsilon P(x, y, z, t), \\ T(x, y, z, t) &= T_b(z) + \varepsilon \Theta(x, y, z, t), \end{aligned} \quad (9)$$

IV. LINEAR STABILITY ANALYSIS

Equations (2) and (3) may be conveniently rewritten according to a pressure–temperature formulation,

where $\varepsilon \ll 1$ is a positive perturbation parameter. The linearisation of the governing equations is carried out by substituting Eq. (9) into Eq. (8) and by neglecting terms $O(\varepsilon^2)$. We thus obtain the governing equations

and boundary conditions for the disturbances, namely

$$\begin{aligned}
a \frac{\partial^2 P}{\partial x^2} + a \frac{\partial^2 P}{\partial y^2} + \frac{\partial^2 P}{\partial z^2} - \frac{R}{a} \frac{\partial \Theta}{\partial z} &= 0, \\
\sigma \frac{\partial \Theta}{\partial t} + Pe \frac{\partial \Theta}{\partial x} - \frac{R}{a} \Theta + \frac{\partial P}{\partial z} &= \frac{\partial^2 \Theta}{\partial x^2} + \frac{\partial^2 \Theta}{\partial y^2} + \frac{\partial^2 \Theta}{\partial z^2}, \\
y = 0, s : \quad \frac{\partial P}{\partial y} &= 0, \quad \frac{\partial \Theta}{\partial y} = 0, \\
z = 0, 1 : \quad \frac{\partial P}{\partial z} &= 0, \quad \Theta = 0.
\end{aligned} \tag{10}$$

Let us now employ the Fourier transforms

$$\begin{aligned}
\tilde{P}(k, y, z, t) &= \frac{1}{\sqrt{2\pi}} \int_{-\infty}^{\infty} P(x, y, z, t) e^{-ikx} dx, \\
\tilde{\Theta}(k, y, z, t) &= \frac{1}{\sqrt{2\pi}} \int_{-\infty}^{\infty} \Theta(x, y, z, t) e^{-ikx} dx,
\end{aligned} \tag{11}$$

in Eq. (10). Then, we obtain a problem where the dependence on the x coordinate is superseded by a parametric dependence on the wavenumber k , namely

$$\begin{aligned}
a \frac{\partial^2 \tilde{P}}{\partial y^2} + \frac{\partial^2 \tilde{P}}{\partial z^2} - a k^2 \tilde{P} - \frac{R}{a} \frac{\partial \tilde{\Theta}}{\partial z} &= 0, \\
\sigma \frac{\partial \tilde{\Theta}}{\partial t} + \left(k^2 - \frac{R}{a} + i k Pe \right) \tilde{\Theta} + \frac{\partial \tilde{P}}{\partial z} &= \frac{\partial^2 \tilde{\Theta}}{\partial y^2} + \frac{\partial^2 \tilde{\Theta}}{\partial z^2}, \\
y = 0, s : \quad \frac{\partial \tilde{P}}{\partial y} &= 0, \quad \frac{\partial \tilde{\Theta}}{\partial y} = 0, \\
z = 0, 1 : \quad \frac{\partial \tilde{P}}{\partial z} &= 0, \quad \tilde{\Theta} = 0.
\end{aligned} \tag{12}$$

The inverse Fourier transforms are reported here for convenience,

$$\begin{aligned}
P(x, y, z, t) &= \frac{1}{\sqrt{2\pi}} \int_{-\infty}^{\infty} \tilde{P}(k, y, z, t) e^{ikx} dk, \\
\Theta(x, y, z, t) &= \frac{1}{\sqrt{2\pi}} \int_{-\infty}^{\infty} \tilde{\Theta}(k, y, z, t) e^{ikx} dk.
\end{aligned} \tag{13}$$

Double Fourier series are employed to formulate the dependence on both y and z for $(\tilde{P}, \tilde{\Theta})$, namely

$$\begin{aligned}
\tilde{P} &= \sum_{n=0}^{\infty} \sum_{m=1}^{\infty} A \cos\left(\frac{n\pi y}{s}\right) \cos(m\pi z) e^{\lambda t}, \\
\tilde{\Theta} &= \sum_{n=0}^{\infty} \sum_{m=1}^{\infty} B \cos\left(\frac{n\pi y}{s}\right) \sin(m\pi z) e^{\lambda t},
\end{aligned} \tag{14}$$

where λ is a complex parameter: the real part of λ is the growth rate of the given Fourier mode while the imaginary part of λ coincides with $-\omega$, where ω is the angular frequency of the given Fourier mode. With Eq. (14), $(\tilde{P}, \tilde{\Theta})$ identically satisfy the boundary conditions reported in Eq. (12). By substituting Eq. (14) into Eq. (12), we obtain two algebraic equations which lead us to an explicit dispersion relation,

$$\sigma \lambda = \frac{R(k^2 + r^2)}{a(k^2 + r^2) + \pi^2 m^2} - (k^2 + r^2 + \pi^2 m^2 + i k Pe), \tag{15}$$

where $r = n\pi/s$ is a real non-negative parameter.

V. MODAL INSTABILITY

The determination of the threshold value of R for the onset of modal, or convective, instability is accomplished through the study the long time behaviour of each single Fourier mode. This is the reason for the term “modal instability”. Thus, the condition of zero growth rate is imposed, *i.e.* $\lambda = -i\omega$. One may define a rescaled angular frequency $\xi = \omega - kPe/\sigma$, where ξ is the angular frequency in the reference frame comoving with the basic flow, so that Eq. (15) yields

$$R = \frac{(k^2 + r^2 + \pi^2 m^2 - i\xi) [a(k^2 + r^2) + \pi^2 m^2]}{k^2 + r^2}. \tag{16}$$

Since R is real, also the right hand side of Eq. (16) must be real. Then, we conclude that $\xi = 0$: the angular frequency in the comoving reference frame of the basic flow is zero and, for this reference frame, the principle of exchange of stabilities holds. Moreover, the Darcy-Rayleigh number simplifies to

$$R = \frac{(k^2 + r^2 + \pi^2 m^2) [a(k^2 + r^2) + \pi^2 m^2]}{k^2 + r^2}. \tag{17}$$

It is worth noting that Eq. (17) agrees with the neutral stability condition reported in the literature⁹, when the Darcy-Rayleigh number is defined by employing the vertical permeability K_z instead of the horizontal permeability K_h . We mention that Storesletten⁹ discusses the stability analysis of the motionless basic state ($Pe = 0$). We emphasise that, exactly as for the Prats’ problem in an isotropic medium⁴, the threshold value for the onset of the modal instability is not affected by the presence of a basic throughflow. This conclusion is easily gathered from Eq. (17).

The neutrally stable Darcy-Rayleigh number R in Eq. (17) is a monotonic increasing function of m . Therefore, for the evaluation of the critical value of R , we can

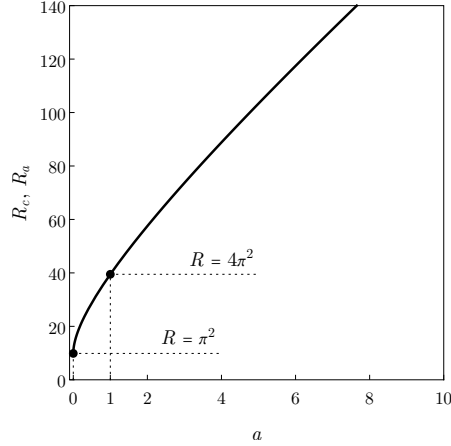


FIG. 2. Threshold value for the onset of modal instability R_c versus a as coincident with the threshold value for the onset of absolute instability R_a for the limiting case $Pe \rightarrow 0$.

set m at its lowest, namely $m = 1$. Then, the minimum of the function $R(\zeta)$, where $\zeta = \sqrt{k^2 + r^2}$, yields the critical values of R and ζ for the onset of the modal instability,

$$R_c = \pi^2 (\sqrt{a+1})^2, \quad \zeta_c = \frac{\pi}{a^{1/4}}. \quad (18)$$

The critical values reported in Eq. (18) coincide with those obtained by Castinel and Combarnous⁶ and reported by Nield and Bejan¹ by considering a vanishing throughflow. For the limiting case of an isotropic porous medium, $a = 1$, Eq. (18) yields the critical values obtained by Prats⁴, $R_c = 4\pi^2$ and $\zeta_c = \pi$. The critical values of R as a function of the parameter a are reported in Fig. 2.

Figure 3 shows the streamlines and isotherms of the perturbation normal modes at critical conditions for $a = 2$, $m = 1$ and $r = 0$. These contour plots reveal that the cells are symmetric with respect to the midplane $z = 1/2$. Compared with the isotropic Darcy–Bénard problem, the shape of the cells is rectangular instead of square. This feature is a consequence of k_c being equal to $\pi/a^{1/4}$.

We note that, for sufficiently large values of r , the minimum value of the neutrally stable R does not coincide with R_c given by Eq. (18). The reason is that, with $r > \pi/a^{1/4}$, the condition $k^2 + r^2 = \zeta_c^2$ cannot be achieved with a real k .

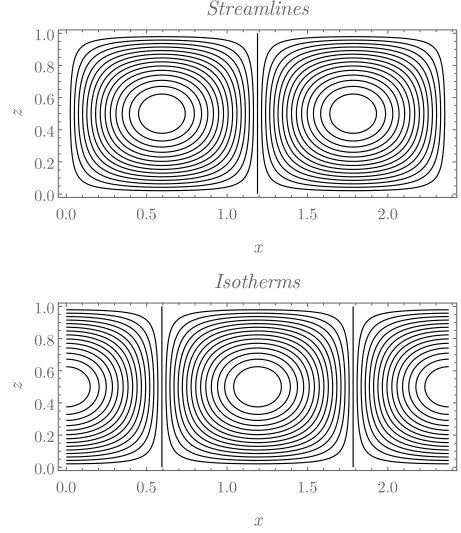


FIG. 3. Streamlines and isotherms for the critical modes with $a = 2$, $m = 1$ and $r = 0$.

VI. ABSOLUTE INSTABILITY

The investigation of the threshold values for the onset of absolute instability aims to study the evolution in time of a wavepacket of Fourier modes, as defined by the inverse Fourier transforms in Eq. (13). This evaluation is carried out by employing the steepest-descent approximation⁵. By using this approximation, the long time behaviour of the integrals in Eq. (13) is determined by the sign of the real part of λ , Eq. (15). More precisely, the condition $\Re\{\lambda(k_0)\} = 0$, where k_0 is a saddle point, *i.e.*, a complex zero of equation $\partial\lambda/\partial k = 0$, identifies the threshold for the onset of absolute instability. For details on this technique, we refer the reader to the book by Barletta⁵. The necessary condition to obtain the correct saddle point for the evaluation of the threshold to absolute instability is the so-called holomorphy requirement. The real k axis can be continuously deformed in the complex k plane to obtain an integration path which crosses the saddle point through a direction of steepest descent. Thus, the region of the complex k plane confined between the deformed integration path and the real k axis cannot include a singularity of $\lambda(k)$ ⁵. Equa-

tion (15) yields

$$\sigma\lambda = \frac{R(k^2 + r^2)}{a(k^2 + r^2) + \pi^2 m^2} - (k^2 + r^2 + \pi^2 m^2 + ikPe),$$

$$\sigma \frac{\partial \lambda}{\partial k} = \frac{2km^2\pi^2 R}{[a(k^2 + r^2) + m^2\pi^2]^2} - 2k - iPe. \quad (19)$$

The function $\lambda(k)$ has the singularities

$$k = \pm i \sqrt{\frac{m^2\pi^2 + ar^2}{a}}. \quad (20)$$

A. The limiting case $Pe \rightarrow 0$

For the limiting case of motionless basic state, $Pe \rightarrow 0$, no unstable Fourier mode can be convected away by the basic flow as the flow rate is zero. The possibility that the basic flow drives away a perturbation growing in time, so that its growth cannot be actually observed by a local measurement of the flow properties, is the physical basis of the distinction between modal and absolute instability²⁰. As a consequence, if $Pe \rightarrow 0$, we expect that the threshold value of the Darcy-Rayleigh number for the onset of absolute instability, R_a , coincides with the critical value, R_c . Therefore, among all the possible saddle points k_0 with $\Re\{\lambda(k_0)\} = 0$, we look for that matching the critical values displayed in Eq. (18). By setting $m = 1$ and $r = 0$, we expect to find a purely real value of k_0 equal to $\pi/a^{1/4}$. For the case of $Pe \rightarrow 0$, the condition $\partial\lambda/\partial k = 0$ yields the following saddle points:

$$k_1 = 0, \quad k_2 = \pm i \sqrt{\frac{\pi^2 + \pi\sqrt{R}}{a}},$$

$$k_3 = \pm i \sqrt{\frac{\pi^2 - \pi\sqrt{R}}{a}}. \quad (21)$$

Because of the singularities reported in Eq. (20), we can exclude the saddle points k_2 . We can exclude also k_1 since it does not match the critical values reported in Eq. (18). By substituting k_3 into the relation $\lambda(k) = 0$, we obtain

$$R_a = \pi^2 (\sqrt{a} + 1)^2, \quad (22)$$

that is what we obtained for the modal stability analysis, as displayed in Eq. (18). By substituting Eq. (22) in Eq. (21) we also obtain $k_3 = \pi/a^{1/4}$, as expected.

For values of the vertical permeability much higher than the values of the horizontal permeability, $K_z \gg K_h$, i.e. for $a \ll 1$, Eq. (22) yields $R_a \rightarrow \pi^2$. On the other

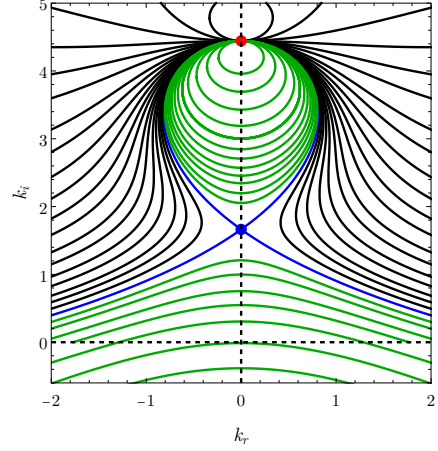


FIG. 4. Holomorphy requirement check in the complex k plane for $a = 0.5$, $m = 1$, $r = 0$ and $Pe = 10$, at the absolute instability threshold $R = R_a = 29.2327$. The blue dot denotes the saddle point, while the red dot denotes the singularity of $\lambda(k)$. The blue lines identify the $\Re\{\lambda\} = 0$ condition, while the black (green) lines are drawn for different positive (negative) values of $\Im\{\lambda\}$.

hand, for $a \gg 1$ and thus for values of horizontal permeability higher than the values of vertical permeability, $K_h \gg K_z$, Eq. (22) yields $R_a \rightarrow \infty$. We can interpret the condition $a < 1$ as one where the vertical flow is favoured so that the buoyancy driven cellular flow onset may happen with smaller values of R . The opposite behaviour is detected when $a > 1$ resulting in a stabilisation of the basic state. In Fig. 2, the threshold value of R for the onset of absolute instability is plotted versus a , for the limiting case $Pe \rightarrow 0$. As already mentioned, this threshold value, R_a , coincides with the critical value, R_c , in this case.

B. Non vanishing flow rate

When the Péclet number is nonzero and a flow rate is present inside the duct, looking for an analytical solution is not a convenient option. The threshold value of the Darcy-Rayleigh number, R_a , is thus obtained by solving numerically the system of algebraic equations

$$\Re\{\lambda\} = 0, \quad \Re\left\{\frac{\partial \lambda}{\partial k}\right\} = 0, \quad \Im\left\{\frac{\partial \lambda}{\partial k}\right\} = 0. \quad (23)$$

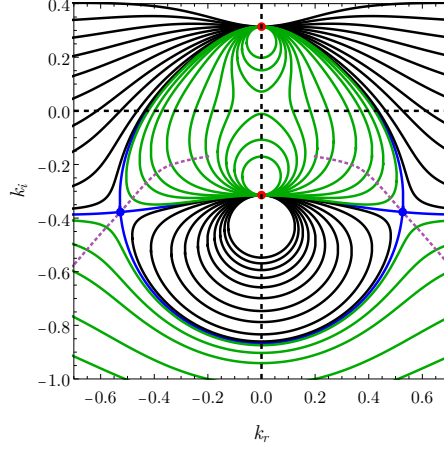


FIG. 5. Holomorphy requirement check in the complex k plane for $m = 1$, $r = 0$, $Pe = 10$ and $a = 100$, with $R = R_a = 1545.47$. The blue dots denote the saddle points, while the red dots denote the singularities of $\lambda(k)$. The blue lines identify the $\Re\{\lambda\} = 0$ condition, while the black (green) lines are isolines of $\Re\{\lambda\}$ drawn for different positive (negative) values of $\Re\{\lambda\}$. The steepest descent paths are identified with purple dotted lines.

For each fixed value of the parameter set (a, m, Pe, r) , there are typically multiple solutions of system (23). We look for the lowest value of R_a constrained by the condition $R_a > R_c$ (absolute instability can arise only if at least one Fourier mode becomes unstable). We also exclude those solutions that require a deformation of the integration path that encloses the singularities reported in Eq. (20). This occurs when the saddle point is purely imaginary, $k_r = 0$, and the absolute value of the imaginary part, k_i , is greater than the absolute value of k evaluated by employing Eq. (20). In these conditions, the singularity is included inside the deformed integration path and, hence, such a solution has to be rejected. Furthermore, some solutions have to be excluded when the steepest-descent path crosses one of the singularities (20). Such a behaviour is illustrated in Fig. 4 for $a = 0.5$, $m = 1$, $r = 0$, $Pe = 10$ at the absolute instability threshold $R = R_a = 29.2327$. This figure displays the singularity with a red dot and the saddle point with a blue dot. The saddle point is located at the intersection of the two blue lines which identify the locus $\Re\{\lambda\} = 0$. The green solid lines are isolines of $\Re\{\lambda\}$ with negative values, while the black solid lines are isolines of $\Re\{\lambda\}$ with positive values. Thus, the paths of steepest descent

departing from the saddle point coincide with the axis $k_r = 0$, so that the upward steepest-descent path crosses the singularity. Such a situation means that the holomorphy requirement is not satisfied.

We present another check of the holomorphy requirement in Fig. 5. It is a case characterised by $m = 1$, $r = 0$, $Pe = 10$ and by $a = 100$. The value of R is the threshold to absolute instability, which is $R_a = 1545.47$. Figure 5 displays the singularities of $\lambda(k)$ as red dots ($k = \pm i\pi/\sqrt{a} = \pm i\pi/10$) and the saddle points as blue dots. The blue, green and black lines have the same meaning as in Fig. 4. The steepest descent paths are denoted as purple dotted lines. Both frames of Fig. 5 report cases where no singularity is to be encircled within the deformed integration paths locally coincident with the steepest-descent paths. Thus, the holomorphy check is to be considered as satisfied.

Figure 6 displays R_a versus Pe for different values of m , r and a . The solid lines denote the modes with $m = 1$, while the dotted lines are relative to $m = 2$. Solid and dotted lines are drawn for different values of the parameter r , namely $r = 0, 2, 5, 10$. Each frame is relative to a different a : $a \rightarrow 0$, $a = 1$, $a = 2$ and $a = 4$. In the frame relative to the limit $a \rightarrow 0$, R_a is independent of Pe and r . Moreover, as a consequence of Eq. (17), R_a coincides with $m^2\pi^2$. In general, we can conclude that R_a is a monotonically increasing function of both m and r . Thus, the transition to absolute instability happens with the lowest possible values of m and r , that is $m = 1$ and $r = 0$.

The most unstable branches of R_a versus Pe (with $m = 1$ and $r = 0$) are plotted in Fig. 7, for different values of the parameter a . For the asymptotic case $a \rightarrow 0$, Fig. 7 shows that R_a is equal to π^2 for every Pe . The dotted line refers to the isotropic case, $a = 1$, and it matches the results obtained by Barletta⁵. We point out that R_a increases with a , for every Pe . This means that the anisotropic permeability of the porous medium implies a destabilisation when $a < 1$ and a stabilisation when $a > 1$. In fact, the destabilising effect of the anisotropy emerges when the permeability in the vertical direction is larger than in the horizontal direction, so that the vertical buoyant flow is favoured. On the other hand, for every fixed a , the threshold R_a is a monotonic increasing function of Pe , exactly as it happens for an isotropic medium⁵. Furthermore, one may note that the dependence on Pe becomes weaker and weaker as a decreases. As already pointed out, in the limit $a \rightarrow 0$, R_a becomes independent of Pe .

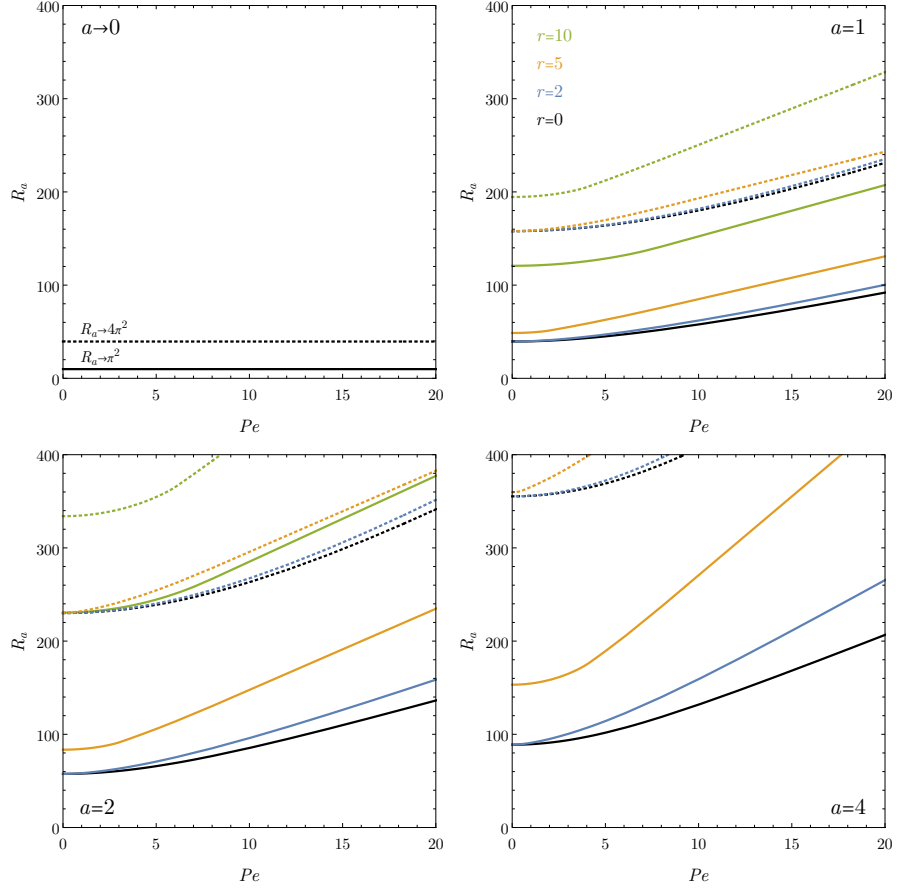


FIG. 6. Threshold values R_a versus Pe for the transition to absolute instability with different values of m , r and a . The solid lines are relative to $m = 1$, while the dotted lines refer to the case $m = 2$. In each frame, the values of r are 0, 2, 5, 10. The four frames correspond to $a \rightarrow 0$, $a = 1$, $a = 2$ and $a = 4$.

VII. CONCLUSIONS

The linear instability of the fluid flow in a saturated horizontal porous duct heated from below has been investigated. Both the onset of the modal instability and its transition to the absolute instability have been studied. The duct has a rectangular cross-section. A basic horizontal throughflow occurs with a dimensionless ve-

locity equal to the Péclet number, Pe . The porous duct considered in the analysis is anisotropic: two different values of permeability, one for the horizontal directions and one for the vertical direction, are assumed. The effect of the anisotropy on the onset of absolute instability has been assessed. The governing parameter that defines the threshold value for the onset of convection is the Darcy-Rayleigh number, R . An exhaustive analysis of the threshold conditions for the onset of modal and

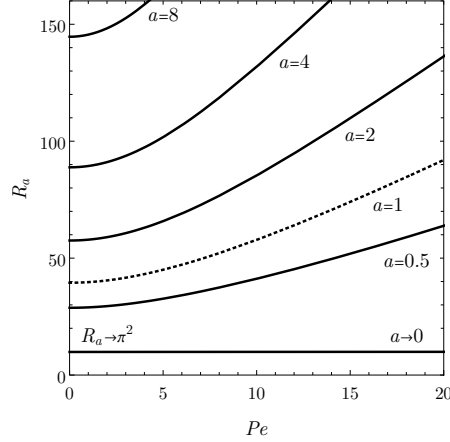


FIG. 7. Values of R_a as a function of Pe for different values of a . The lines are drawn for the most unstable set of the parameters $(m, r) = (1, 0)$. The dotted line refers to the isotropic case $a = 1$.

absolute instability has been carried out leading to the following conclusions:

- As for the Prats problem, the threshold for the onset of modal instability is not affected by the presence of a horizontal throughflow: the critical values for the onset of modal instability match those reported in the literature for the Horton–Rogers–Lapwood problem within an anisotropic porous medium.
- The principle of exchange of stabilities holds for the reference frame comoving with the basic throughflow.
- The threshold value of the Darcy–Rayleigh number for the transition to absolute instability is a monotonic increasing function of the Péclet number. Thus, the basic throughflow turns out to display a stabilising effect when it comes to absolute instability.
- In the transition to absolute instability, the threshold value of the Darcy–Rayleigh number, R_a , is a monotonic increasing function of the ratio between the value of the permeability for the horizontal plane and the value of the permeability for the vertical direction. In other words, the vertical permeability has a destabilising effect on the basic state while the horizontal permeability has a stabilising effect.

- The lowest possible value of the Darcy–Rayleigh number for the onset of absolute instability is $R_a \rightarrow \pi^2$, and it is attained when the ratio between the horizontal permeability and the vertical permeability tends to zero.

The analysis carried out in this paper accounts for the simplest situation where anisotropy emerges. There are more general cases where there can be two different horizontal permeabilities, or the three principal axes of the permeability tensor can be inclined to the horizontal. In such cases, there are more dimensionless parameters governing the anisotropy and, hence, the transition to absolute instability. Despite the increased difficulty, such a generalised scenario can be quite interesting for practical applications regarding, especially, the dynamics of hot groundwater and it will be definitely an opportunity for future research in this field.

ACKNOWLEDGMENTS

The authors acknowledge the financial support from Grant No. PRIN 2017F7KZWS provided by the Italian Ministero dell’Istruzione, dell’Università e della Ricerca.

AUTHOR DECLARATIONS

Conflict of Interest

The authors have no conflicts of interest to disclose.

DATA AVAILABILITY STATEMENT

The data that support the findings of this study are available within the article.

¹D. A. Nield and A. Bejan, *Convection in porous media*, 5th ed. (Springer, New York, 2017).

²C. W. Horton and F. T. Rogers Jr, “Convection currents in a porous medium,” *Journal of Applied Physics* **16**, 367–370 (1945).

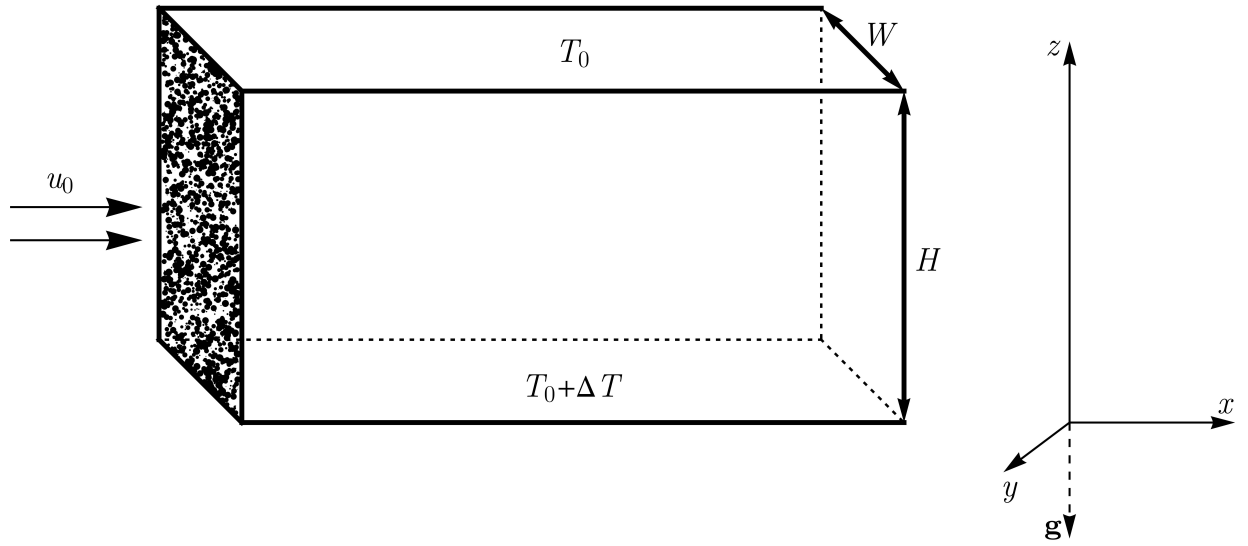
³E. R. Lapwood, “Convection of a fluid in a porous medium,” *Mathematical Proceedings of the Cambridge Philosophical Society* **44**, 508–521 (1948).

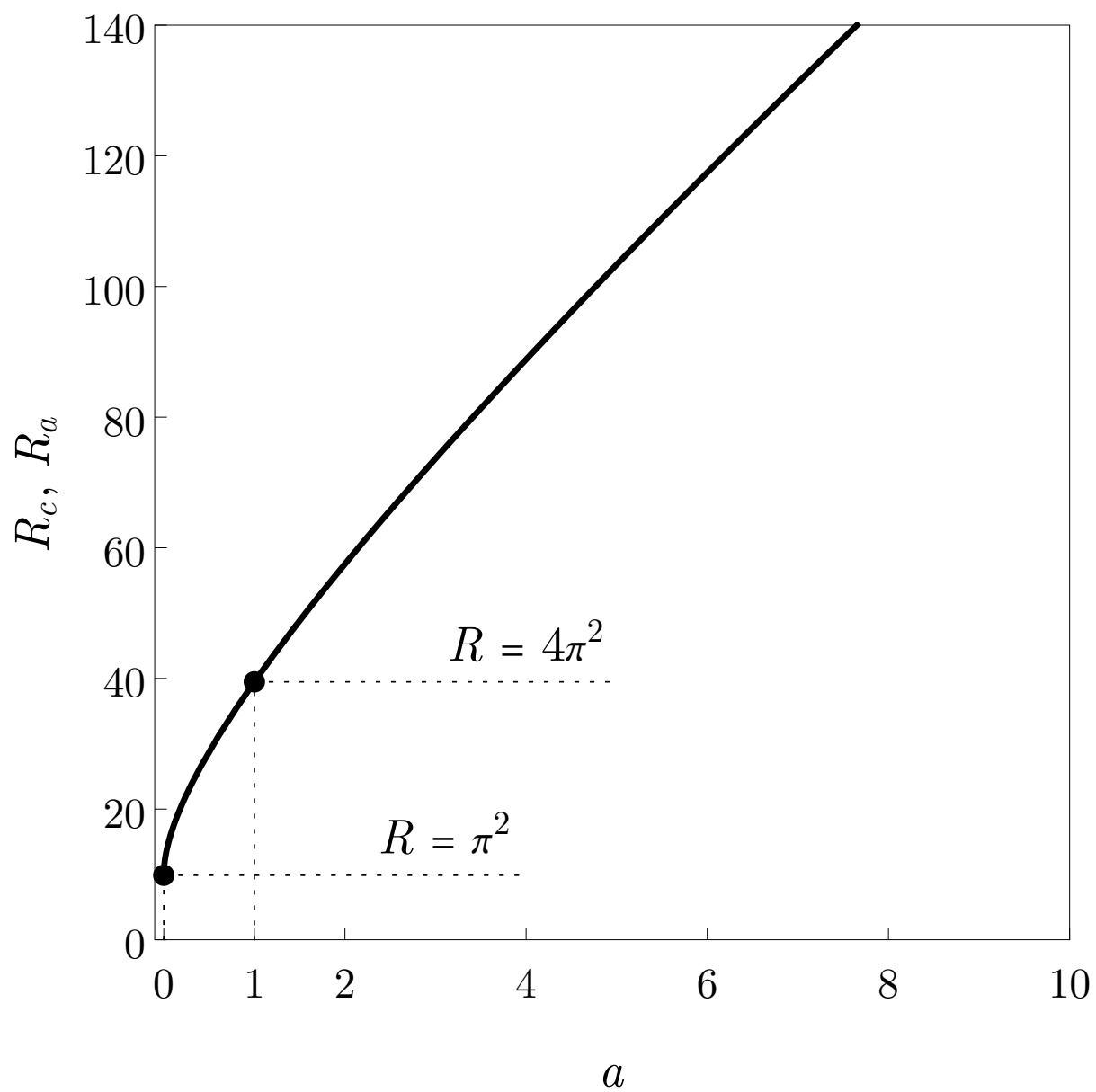
⁴M. Prats, “The effect of horizontal fluid flow on thermally induced convection currents in porous mediums,” *Journal of Geophysical Research* **71**, 4835–4838 (1966).

⁵A. Barletta, *Routes to Absolute Instability in Porous Media* (Springer, 2019).

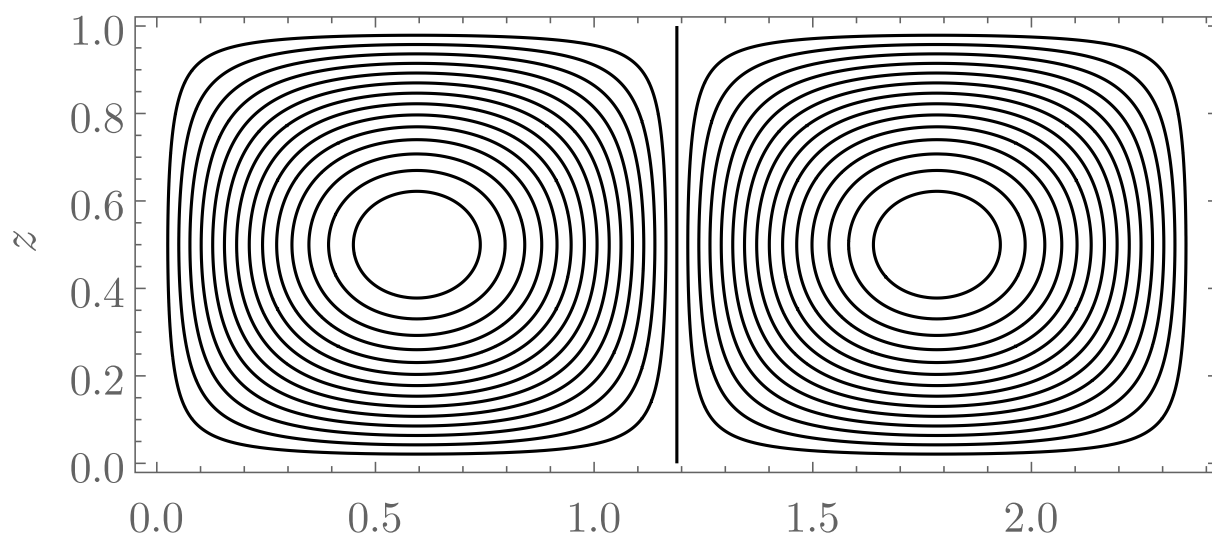
⁶G. Castinel and M. Combarous, “Critère d’apparition de la convection naturelle dans une couche poreuse anisotrope horizontale,” *Comptes Rendus de l’Académie des Sciences, Série B* **287**, 701–704 (1974).

- ⁷R. McKibbin, "Thermal convection in a porous layer: effects of anisotropy and surface boundary conditions," *Transport in Porous Media* **1**, 271–292 (1986).
- ⁸Y. Qin and P. N. Kaloni, "Convective instabilities in anisotropic porous media," *Studies in Applied Mathematics* **91**, 189–204 (1994).
- ⁹L. Storesletten, "Effects of anisotropy on convective flow through porous media," in *Transport Phenomena in Porous Media*, edited by D. B. Ingham and I. Pop (Pergamon Press Oxford, 1998) pp. 261–283.
- ¹⁰A. Postelnicu and D. A. S. Rees, "The onset of convection in an anisotropic porous layer inclined at a small angle from the horizontal," *International Communications in Heat and Mass Transfer* **28**, 641–650 (2001).
- ¹¹D. A. S. Rees and A. Postelnicu, "The onset of convection in an inclined anisotropic porous layer," *International Journal of Heat and Mass Transfer* **44**, 4127–4138 (2001).
- ¹²D. A. S. Rees, L. Storesletten, and A. Postelnicu, "The onset of convection in an inclined anisotropic porous layer with oblique principle axes," *Transport in Porous Media* **62**, 139–156 (2006).
- ¹³L. Storesletten and D. A. S. Rees, "Onset of convection in an inclined anisotropic porous layer with internal heat generation," *Fluids* **4**, 75 (2019).
- ¹⁴D. A. S. Rees, L. Storesletten, and A. P. Bassom, "Convective plume paths in anisotropic porous media," *Transport in Porous Media* **49**, 9–25 (2002).
- ¹⁵J. Ennis-King, I. Preston, and L. Paterson, "Onset of convection in anisotropic porous media subject to a rapid change in boundary conditions," *Physics of Fluids* **17**, 084107 (2005).
- ¹⁶D. A. Nield and A. V. Kuznetsov, "The effects of combined horizontal and vertical heterogeneity and anisotropy on the onset of convection in a porous medium," *International Journal of Thermal Sciences* **46**, 1211–1218 (2007).
- ¹⁷M. De Paoli, F. Zonta, and A. Soldati, "Influence of anisotropic permeability on convection in porous media: Implications for geological CO₂ sequestration," *Physics of Fluids* **28**, 056601 (2016).
- ¹⁸C. Beckermann and R. Viskanta, "Forced convection boundary layer flow and heat transfer along a flat plate embedded in a porous medium," *International Journal of Heat and Mass Transfer* **30**, 1547–1551 (1987).
- ¹⁹K. Vafai and S. J. Kim, "Forced convection in a channel filled with a porous medium: an exact solution," *ASME Journal of Heat Transfer* **111**, 1103–1106 (1989).
- ²⁰P. Huerre and P. A. Monkewitz, "Absolute and convective instabilities in free shear layers," *Journal of Fluid Mechanics* **159**, 151–168 (1985).
- ²¹A. Barletta and L. Storesletten, "Thermoconvective instabilities in an inclined porous channel heated from below," *International Journal of Heat and Mass Transfer* **54**, 2724–2733 (2011).
- ²²D. A. S. Rees and A. P. Bassom, "The onset of Darcy-Bénard convection in an inclined layer heated from below," *Acta Mechanica* **144**, 103–118 (2000).
- ²³A. Barletta and D. A. S. Rees, "Linear instability of the Darcy-Hadley flow in an inclined porous layer," *Physics of Fluids* **24**, 074104 (2012).
- ²⁴A. Barletta and D. A. S. Rees, "Local thermal non-equilibrium analysis of the thermoconvective instability in an inclined porous layer," *International Journal of Heat and Mass Transfer* **83**, 327–336 (2015).
- ²⁵L. A. Sphaier, A. Barletta, and M. Celli, "Unstable mixed convection in a heated inclined porous channel," *Journal of Fluid Mechanics* **778**, 428–450 (2015).
- ²⁶A. Barletta, "A proof that convection in a porous vertical slab may be unstable," *Journal of Fluid Mechanics* **770**, 273–288 (2015).
- ²⁷A. E. Gill, "A proof that convection in a porous vertical slab is stable," *Journal of Fluid Mechanics* **35**, 545–547 (1969).
- ²⁸D. A. Nield, "Onset of thermohaline convection in a porous medium," *Water Resources Research* **4**, 553–560 (1968).
- ²⁹D. A. S. Rees and A. Barletta, "Linear instability of the isoflux Darcy-Bénard problem in an inclined porous layer," *Transport in Porous Media* **87**, 665–678 (2011).





Streamlines



Isotherms

